



# TPD of $\text{NO}_2^-$ and $\text{NO}_3^-$ from Na-Y: The relative stabilities of nitrates and nitrites in low temperature DeNOx catalysis

Aditya Savara, Wolfgang M.H. Sachtler, Eric Weitz \*

Department of Chemistry and Institute for Catalysis in Energy Processes, Northwestern University, 2145 Sheridan Road, Evanston, IL 60208-3113, United States

## ARTICLE INFO

### Article history:

Received 2 December 2008  
Received in revised form 17 February 2009  
Accepted 27 February 2009  
Available online 13 March 2009

### Keywords:

DeNOx  
Nitrate  
Nitrite  
TPD  
Zeolite

## ABSTRACT

Temperature programmed depletion (TPD) was performed for both surface nitrates ( $\text{H}^+ - \text{NO}_3^-$ ) and surface nitrites ( $\text{H}^+ - \text{NO}_2^-$ ) on Na-Y. The depletion curves are each adequately described with a pre-exponential of  $10^{13}$  and activation energies that vary as a function of coverage from  $\sim 100$  to  $200 \text{ kJ mol}^{-1}$ . Multiple adsorption sites could lead to the observed variation in activation energies.  $\text{NO}_2^-$  is more kinetically stable than  $\text{NO}_3^-$  on Na-Y. The effect that the method of preparation of  $\text{NO}_3^-$  and  $\text{NO}_2^-$  could have on the relative stabilities of the nitrates and nitrites is discussed. The trends for the relative stabilities of different nitrates and nitrites on Na-Y and BaNa-Y are examined as a function of the cationic adsorption site and the counter-ion (e.g.,  $\text{H}^+$  and  $\text{NO}^+$ ). The possible roles of the stabilities of nitrates and nitrites in low temperature DeNOx catalysis are considered.

© 2009 Elsevier B.V. All rights reserved.

## 1. Introduction

The chemistry involved in low temperature ( $<250^\circ\text{C}$ ) abatement of nitrogen oxides (DeNOx) is of both scientific and societal interest, particularly for diesel vehicle exhaust [1–3]. One strategy for low temperature NOx removal is selective catalytic reduction (SCR) with added reductants [1,2]. It was recently found that Na-Y zeolites that have been exchanged with a series of alkali or alkaline metal cations are very efficient catalysts for NOx SCR with either  $\text{NH}_3$  or added organic oxygenates as a reductant [4–7]. Mechanistic studies have shown that reactions of added organic oxygenates can lead to *in situ* production of  $\text{NH}_3$ , which then acts as the reductant for NOx [5,6].

Within the aforementioned series, BaNa-Y is the most active DeNOx catalyst [8]. However, the reasons behind the superiority of  $\text{Ba}^{2+}$  versus other cations are not yet well understood. One possible cause of the superior performance of BaNa-Y could be related to the relative stabilities of surface nitrates and surface nitrites that are formed as intermediates during DeNOx catalysis [9]. To gain insight into this issue, we have performed temperature programmed depletion (TPD) experiments on Na-Y, and will discuss how the relative stabilities of the nitrates and nitrites on Na-Y compare to those on BaNa-Y. The term “depletion” is used in preference to “desorption” as studies have not yet shown whether

the nitrates desorb first or decompose first as they leave the surface [10,11].

The surface nitrates and nitrites used in this study have  $\text{H}^+$  as the counter-ion, which is discussed in Section 4.3.

## 2. Experimental

Na-Y was obtained from Aldrich (#334448, Si/Al  $\sim 2.5$ ). The Si/Al ratio of 2.62 was determined by inductively coupled plasma (ICP) atomic emission spectroscopy. A thin film of 10–50 mg Na-Y zeolite was “painted” onto a tungsten grid, and mounted in a home-built IR cell, which is described in detail elsewhere [5,12]. This cell allows for controlled heating (under vacuum) of the tungsten grid supporting the catalyst sample. Surface species were monitored by an FTIR spectrometer operated in transmission mode. The standard tangential base-line method was used for integration of surface nitrate and nitrite peaks [13,14], with areas integrated from 1500 to  $1360 \text{ cm}^{-1}$  and from 1300 to  $1250 \text{ cm}^{-1}$ , respectively. The surface nitrate and surface nitrite peaks on Na-Y span from approximately 1500 to  $1300 \text{ cm}^{-1}$  and 1350 to  $1200 \text{ cm}^{-1}$ , respectively; with peak centers at approximately 1400 and  $1270 \text{ cm}^{-1}$ , respectively; in good agreement with literature values [11,15–19]. Integrated areas of IR absorbance peaks were used for quantitative measurements of the surface nitrates and nitrites.

Prior to each TPD experiment, the Na-Y sample was heated at  $430^\circ\text{C}$  for 3–4 h at a pressure of  $\leq 10^{-4}$  Torr to remove adsorbed water. The Na-Y was then allowed to cool to the initial TPD

\* Corresponding author. Tel.: +1 847 491 5583; fax: +1 847 491 7713.  
E-mail address: [weitz@northwestern.edu](mailto:weitz@northwestern.edu) (E. Weitz).

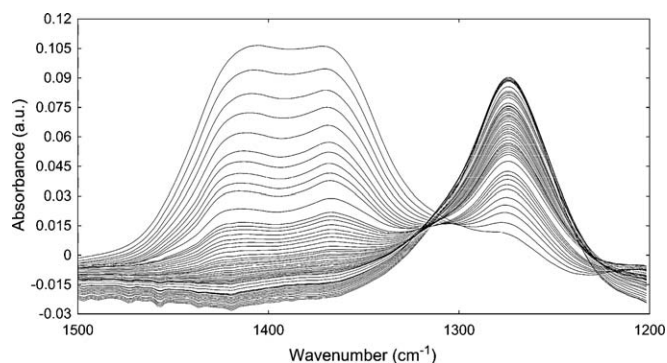


**Fig. 1.** IR spectra displaying the conversion of surface nitrates (peak centered at  $\sim 1400\text{ cm}^{-1}$ ) to surface nitrites (peak centered at  $\sim 1270\text{ cm}^{-1}$ ) on Na-Y, produced by exposure of  $\sim 0.2\text{ Torr NO}_2$  at  $150^\circ\text{C}$ . Spectra were taken every 30 s.

temperature ( $T_0$ ), and maintained at that temperature under vacuum for at least 1 h prior to subsequent experiments. Surface nitrates were produced on Na-Y by introduction of excess gas phase nitric acid. Upon saturation of the adsorption sites (no further growth of the surface nitrate IR peak), the reactor was evacuated for several min at a pressure of  $<10^{-2}\text{ Torr}$  to remove residual  $\text{HNO}_3$  vapor and any weakly bound surface nitrates. Nitrites were produced on the Na-Y surface by either: (a) first forming nitrates on the surface as described above, followed by introduction of NO to reduce the nitrates to nitrites [20], or (b) simply by introduction of  $\text{NO}_2$  instead of nitric acid, as  $\text{NO}_2$  has been observed to produce nitrites on Na-Y [18]. It is possible that the latter method also produces some nitrites due to reduction of nitrates by NO (always present in equilibrium when  $\text{NO}_2$  is present). The kinetics of the reduction of surface nitrates by NO on BaNa-Y and Na-Y is the topic of a publication currently in preparation. Nitrites produced by each of these methods have similar behavior during TPD experiments, and in our discussions of the adsorption we will not differentiate between them. The conversion of nitrates to nitrites on Na-Y, subsequent to introduction of  $\text{NO}_2$  at  $150^\circ\text{C}$ , is shown in Fig. 1. An isobestic point is observed at  $\sim 1310\text{ cm}^{-1}$ , corresponding to the conversion of nitrates to nitrites. The isobestic point is not a “perfect point” due to a gradual baseline shift that takes place as the surface nitrate coverage changes. We attribute this shift in the baseline to changes in the infrared absorption of the zeolite framework bands as a result of interactions with the surface nitrates [21]. Peak areas were normalized to the maximum peak area observed prior to TPD, resulting in a unitless relative coverage,  $\theta$ , with an initial coverage of  $\theta_0$ . FTIR scans were taken 1 min apart with a heating rate,  $\beta_H$ , of either 3 or  $5^\circ\text{C/min}$ . The conditions for surface nitrate TPD ( $T_0$ ,  $\theta_0$ ,  $\beta_H$ ) were: ( $150^\circ\text{C}$ , 0.99,  $3^\circ\text{C/min}$ ); ( $50^\circ\text{C}$ , 0.92,  $5^\circ\text{C/min}$ ); ( $50^\circ\text{C}$ , 0.91,  $5^\circ\text{C/min}$ ). The conditions for the surface nitrite TPD ( $T_0$ ,  $\theta_0$ ,  $\beta$ ) were: ( $150^\circ\text{C}$ , 1.00,  $3^\circ\text{C/min}$ ); ( $150^\circ\text{C}$ , 0.91,  $3^\circ\text{C/min}$ ); ( $150^\circ\text{C}$ , 0.68,  $3^\circ\text{C/min}$ ).

### 3. Results and Analysis

Typical depletion curves for surface nitrates and surface nitrites on Na-Y are shown in Fig. 2 ( $\theta$  vs.  $T$ ).

The change in  $\theta$  with temperature ( $d\theta/dT$ ) did not have a maximum (no TPD “peak”) when plotted as a function of temperature, for either the surface nitrate or surface nitrite TPD depletion curves in Fig. 2. Without a peak in the TPD data, a “Redhead analysis” of the TPD data was not possible [22]. Instead, a TPD analysis of the King/Taylor–Weinberg variety was performed with an assumed and constant pre-exponential [22].

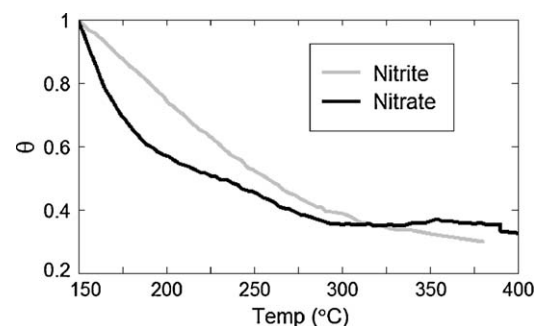


**Fig. 2.** Depletion curves for surface nitrates and surface nitrites on Na-Y.

The rate constant for desorption or reactive depletion of surface entities can be found from the expression [22]:

$$k_0 \exp\left(\frac{-E_A}{RT}\right) = -\frac{d\theta}{dT} \left(\frac{1}{\theta^n}\right) \beta_H \quad (1)$$

where  $k_0$  is the pre-exponential factor for desorption,  $E_A$  is the activation energy for desorption,  $n$  is the order of the reaction,  $\beta_H$  is the heating rate, and the other variables have their usual meanings. As mentioned above,  $k_0$  was assumed to be constant while the activation energy was allowed to vary as a function of coverage; a common assumption ( $E_A$  is then a function of  $\theta$ ) [23–25]. Due to the degree of freedom introduced by allowing the activation energy to vary as a function of coverage, it was not possible to definitively determine whether desorption was first or second order in  $\theta$  (i.e., a change in the rate due to reaction order could be compensated for by a change in the activation energy as a function of coverage). The units of  $k_0$  are the same for either a first-order or second-order surface process ( $\text{s}^{-1}$ ) when the concentration is expressed as  $\theta$  (which is unitless), with typical pre-exponentials being on the order of  $10^{13}\text{ s}^{-1}$  [26]. Using Eq. (1), and assuming a first order process, with  $k_0 = 10^{13}\text{ s}^{-1}$  [26,27], yields the curves for the activation energy that are shown in Fig. 3a. Using Eq. (1) for a second-order process with  $k_0 = 10^{13}\text{ s}^{-1}$  [26], yields the activation energy curves shown in Fig. 3b. The small discontinuities observed in Fig. 3 (e.g., at  $\theta = 0.67$  for the nitrites) are within experimental errors, however the averaging of a limited number of curves (three) from separate TPD experiments after spline fitting also contributes to these deviation. With the choice of  $k_0 = 10^{13}\text{ s}^{-1}$ , the range of activation energies (the difference between the maximum and the minimum) obtained is  $\sim 100\text{ kJ mol}^{-1}$ . As shown in the Supplementary Material, for any realistic pre-exponential,  $10^{10}\text{ s}^{-1} < k_0 < 10^{18}\text{ s}^{-1}$  [26,28,29], the range of the activation energies that are obtained is  $>50\text{ kJ mol}^{-1}$  for both the nitrates and the nitrites. Additionally, the curves in Fig. 3 would be qualitatively similar regardless of the pre-exponential chosen, although they may be vertically shifted and stretched on the order of 20–50  $\text{kJ mol}^{-1}$  (shown in the Supplementary Material). However, we note that since the experimentally determined rate of nitrate depletion was greater than the rate of nitrite depletion for all  $\theta$ , the nitrite is kinetically more stable.

### 4. Discussion

#### 4.1. TPD results and site heterogeneity

Prior TPD experiments with nitrates or nitrites on Na-Y and related catalysts have not attempted to characterize the details of the desorption kinetics. We note that the curves obtained in Fig. 3 are very similar for  $n = 1$  and  $n = 2$ . As indicated above, a coverage dependent activation energy can effectively compensate for the

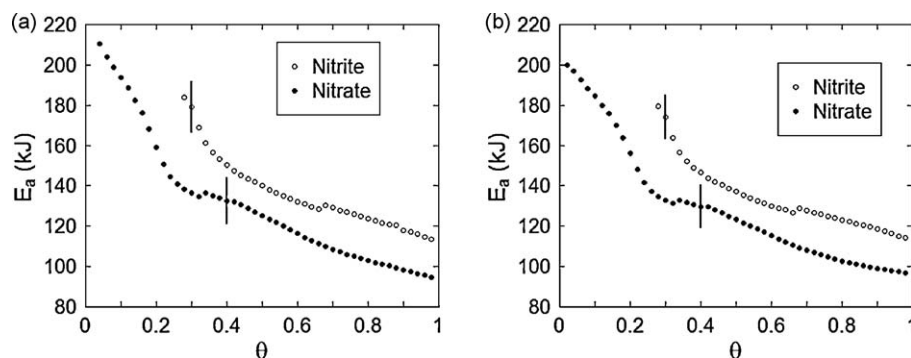


**Fig. 3.** Activation energy for depletion as a function of theta assuming a pre-exponential of  $10^{13} \text{ s}^{-1}$ , for surface nitrates and surface nitrites on Na-Y. (a)  $n = 1$ , first-order; (b)  $n = 2$ , second-order. The two representative error bars shown are the standard deviations at those points, based on multiple TPD experiments.

difference in the coverage dependence of the rate equation on order (i.e., for  $n = 1$  vs.  $n = 2$ ). The similarity observed between the curves in Fig. 3 is due to the strong dependence of the rate on the activation energy, which is much greater than the dependence of the rate on coverage (i.e.,  $n = 1$  vs.  $n = 2$  in the rate equation) [22]. Thus, only a small change in the activation energy curve is needed to compensate for the different coverage dependences for  $n = 1$  and  $n = 2$  processes.

An observed decrease in activation energy with increasing total coverage is common for TPD from surfaces, and is often explained by adsorption at multiple sites [22,24,30–32]. The general trend – a steep decrease in the activation energy followed by a shallower decrease in the activation energy, with increasing coverage – and the order of magnitude of variation for  $E_a$  with coverage (50–150  $\text{kJ mol}^{-1}$ ) displayed in Fig. 3 are both consistent with similar trends observed in the literature for adsorption on zeolites [30–34], which have been ascribed to adsorption on multiple crystallographic sites within the zeolite [35,36], as opposed to adsorbate–adsorbate interactions. However, adsorbate–adsorbate interactions could contribute to the observed trend.

#### 4.2. Relative stability of $\text{NO}_3^-$ and $\text{NO}_2^-$ on Na-Y

For all coverages, the depletion rate of the nitrates on Na-Y was greater than that of the depletion rate of the nitrites, indicating that the chemisorbed nitrites are kinetically more stable. This result is in contrast to the TPD results of Sedlmair et al., who reported that the nitrates on Na-Y were kinetically more stable [37]. Sedlmair et al. inferred that the chemisorbed nitrates were also thermodynamically more stable than the chemisorbed nitrites on Na-Y [37].

However, in the work published by Sedlmair et al. and in other studies [17,18,37], the nitrates and nitrites were produced without an attempt to favor production of one species over the other, and both thus coexisted on the zeolite surface. Yet, both species are believed to occupy the same type of sites [11,17,20]. Only in the present study were nitrates prepared independently, and in separate experiments nitrates were *intentionally converted to nitrites*, by exposure to NO prior to TPD. The rationale being that NO is known to convert chemisorbed nitrates to nitrites on these catalysts [20], and we directly observed this conversion in our experiments.

Sedlmair et al. likewise prepared nitrates and nitrites by exposure to NO; however they used a preparation temperature of 50 °C. The reaction time at 50 °C was insufficient to reduce all nitrates to nitrites, as the majority of nitrates were still present after NO exposure [37]. Under such circumstances it is plausible that only the most weakly adsorbed nitrates would be reduced by NO (which is also always in equilibrium with  $\text{NO}_2$  when  $\text{NO}_2$  is present) [20]. Thus, differences in preparation methods could play

a role in the reported differences in nitrate versus nitrite stabilities on Na-Y. However, the nitrates and nitrites on Na-Y have very similar stabilities, and reports in the literature indicate that binding energies can vary from one zeolite sample to another [38,39]—thus it is possible that the order of their stabilities could reverse in experiments done on different batches of Na-Y.

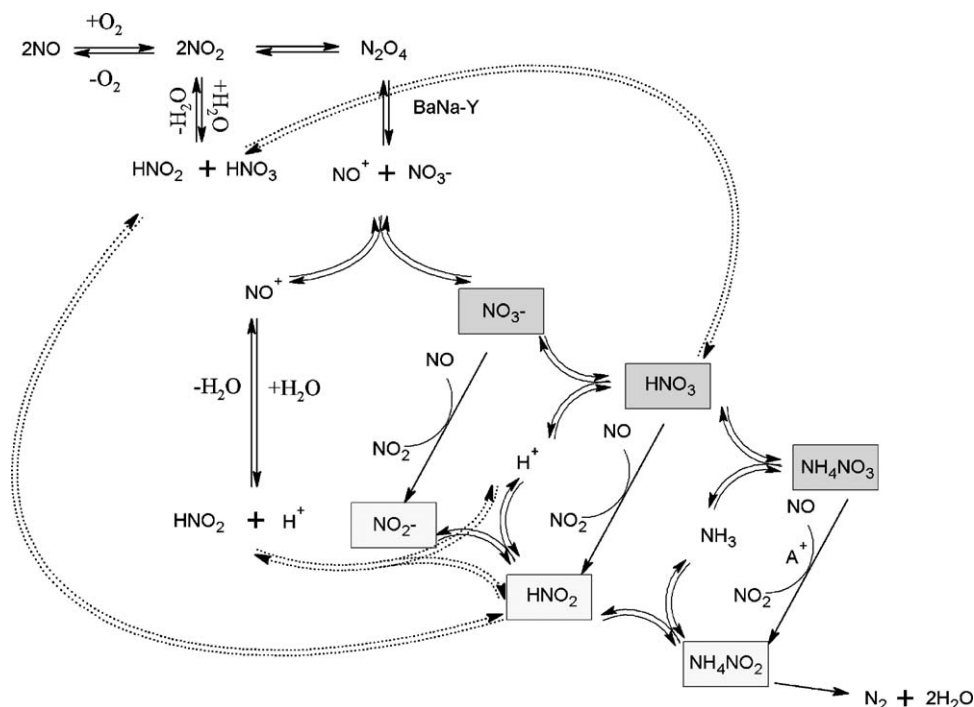
It is not possible to clarify from our experiments whether the source of the differing results is due to different sample preparation methods or inherent differences in the samples themselves. Such clarification would require additional experiments with the samples used by Sedlmair et al., in which the nitrates are exposed to NO at higher temperatures prior to TPD (temperatures comparable to those used during this study), in an attempt to convert even the most strongly bound nitrates to nitrites prior to TPD.

The discussion above suggests that the preparation of the surface species could result in different relative occupations of sites, which can affect the observed kinetic stabilities, and thus the inferred thermodynamic stabilities.<sup>1</sup> As mentioned, the zeolite samples in the cited studies [17,18,37] were obtained from different sources and/or used different ion-exchange procedures, which may also play a role in the different reported stabilities. The role of the preparation of a given zeolite sample in altering the desorption activation energies for these species has not been systematically studied.

#### 4.3. Stability of $\text{NO}_3^-$ and $\text{NO}_2^-$ on Na-Y versus BaNa-Y

As discussed in Section 1, BaNa-Y is a superior catalyst for NOx reduction relative to Na-Y that has been ion-exchanged with other alkali or alkaline earth metal cations. Experimental complications make it difficult to perform TPD on surface nitrites on BaNa-Y (discussed in the [Supplementary Material](#)), though the activation energy for desorption can be estimated [22] as  $< \sim 100 \text{ kJ mol}^{-1}$  based on the temperatures at which these surface nitrites decompose ( $< 100^\circ\text{C}$ ) [20] and assuming a pre-exponential of  $> 10^{13}$  [26,28,29]. In previous work, we performed TPD of surface nitrates on BaNa-Y, and found that the activation energy for depletion was likely in the range of 160–200  $\text{kJ mol}^{-1}$  for most of the surface nitrates, while a minority of the surface nitrates on BaNa-Y were significantly more stable (i.e., having an activation energy for depletion of  $> 200 \text{ kJ mol}^{-1}$ ) [10]. These activation energies for depletion of nitrates and nitrites on BaNa-Y can be compared to the corresponding values for Na-Y, to gain insight into the reasons for the superior performance of BaNa-Y in low temperature DeNOx catalysis.

<sup>1</sup> A brief discussion regarding issues involved in inferring the thermodynamic stabilities of chemisorbed nitrates and nitrites from studies on desorption kinetics is included in the [Supplementary Material](#).



Scheme 1.

One possible cause of the superior performance of BaNa-Y could be the relative stabilities of the surface nitrates and nitrites which are produced as intermediates during DeNO<sub>x</sub> catalysis. These surface intermediates are chemisorbed on the extra-framework cations; and it has been shown that reduction of the surface nitrates to nitrites plays an important role in DeNO<sub>x</sub> catalysis over BaNa-Y [20]. When NH<sub>3</sub> is produced *in situ*, or introduced as part of the reactant stream, the primary routes to N<sub>2</sub> over BaNa-Y at 200 °C are shown in Scheme 1 [9].<sup>2</sup> As can be seen on the right-hand side of Scheme 1, the nitrates (NO<sub>3</sub><sup>-</sup>, HNO<sub>3</sub>, NH<sub>4</sub>NO<sub>3</sub>) are reduced to their corresponding nitrites (NO<sub>2</sub><sup>-</sup>, HNO<sub>2</sub>, NH<sub>4</sub>NO<sub>2</sub>) by NO. Finally, NH<sub>4</sub>NO<sub>2</sub> is the key intermediate which rapidly decomposes to N<sub>2</sub> and H<sub>2</sub>O above 100 °C [40]. Similar mechanisms have been proposed for NO<sub>x</sub> SCR with NH<sub>3</sub> as the reductant over Fe-ZSM-5 [41,42], and V<sub>2</sub>O<sub>5</sub>-WO<sub>3</sub>/TiO<sub>2</sub> [3,43–45].

Any nitrite (lightly shaded boxes) produced from the reduction of a nitrate (darkly shaded boxes) by NO must be neither too stable nor too unstable, otherwise reaction will not proceed through the desired mechanistic pathway (to NH<sub>4</sub>NO<sub>2</sub>), according to the Sabatier principle [28]. Our previous studies [20,46] have shown that reduction of NO<sub>3</sub><sup>-</sup> and NH<sub>4</sub>NO<sub>3</sub> by NO converts species that would otherwise be potential catalyst deactivators on BaNa-Y into desired intermediates. Thus, the stabilities and reactivities of the nitrates and nitrites could be an important factor in determining the efficiencies of NO<sub>x</sub> reduction over this series of catalysts. Our studies also suggest that on BaNa-Y the kinetically favored route to NH<sub>4</sub>NO<sub>2</sub> at 200 °C goes through NO<sub>3</sub><sup>-</sup> which is reduced to NO<sub>2</sub><sup>-</sup> [20]. The same key steps have been proposed on Fe-ZSM-5 [41].

The factors which control the stabilities of nitrates and nitrites on these catalysts are not yet completely understood. As discussed in the Supplementary Material, there have been differences in the

findings among different groups for the stabilities of the surface species produced from the adsorption of NO<sub>x</sub> on these catalysts. However, some general qualitative trends for the stabilities of NO<sub>2</sub><sup>-</sup> and NO<sub>3</sub><sup>-</sup> can be deduced from the literature [5,11,17–20,37,38,40,46–61], showing that desorption/decomposition temperatures are consistent to within about 50–100 °C. These trends are shown in Fig. 4, which includes the results of this study for H<sup>+</sup>–(NO<sub>2</sub><sup>-</sup>)–Na-Y and H<sup>+</sup>–(NO<sub>3</sub><sup>-</sup>)–Na-Y (see Supplementary Material for a more detailed table of the information used to make Fig. 4). Zeolite frameworks often have Al<sup>3+</sup> defect sites [62]; the stabilities of the nitrates and nitrites on these Al<sup>3+</sup> sites have also been included in Fig. 4. The resulting trends for the stabilities of nitrates and nitrites on this series of zeolite catalysts can be summarized as follows:

1. Nitrates are typically more stable than nitrites.
2. When H<sup>+</sup> is the counter-ion, nitrates and nitrites are both more stable than when NO<sup>+</sup> is the counter-ion.
3. The relative stabilities among nitrates and nitrites depend on the adsorption site, with the order being: Ba<sup>2+</sup> > Na<sup>+</sup> > Al<sup>3+</sup>.

H<sup>+</sup>–(NO<sub>2</sub><sup>-</sup>)–Na-Y is shown as slightly more stable than H<sup>+</sup>–(NO<sub>3</sub><sup>-</sup>)–Na-Y in Fig. 4 to correspond with the results of the present study.

It should be noted that the effect of the cation on the stabilities of nitrate and nitrite complexes with Ba<sup>2+</sup> and Na<sup>+</sup> are *inverted* for the zeolite with respect to in the bulk salts: in the bulk the Na<sup>+</sup>-coordinated species are more stable, while for these zeolites the Ba<sup>2+</sup>-coordinated species are more stable. Presumably, coordination in the zeolite environment changes the hardness/softness of the cations and anions, making the hardness/softness of Ba<sup>2+</sup> a better match than that of Na<sup>+</sup> for these anions, consistent with application of the hard and soft acid and base principle (HSAB) within the zeolite environment [63–65]. The charge density of the extra-framework cation is likely the largest factor in the hardness of the extra-framework cation [66], and has also been correlated with the activity of these catalysts. It has been shown that the charge density of the extra-framework cation is inversely

<sup>2</sup> The reduction of NH<sub>4</sub>NO<sub>3</sub> by NO is acid catalyzed [46]. We note that the reaction of NO<sub>2</sub> with water [69–71]: 2NO<sub>2</sub> + H<sub>2</sub>O → HNO<sub>2</sub> + HNO<sub>3</sub> can be followed by 2HNO<sub>2</sub> → NO<sub>2</sub> + NO + H<sub>2</sub>O [71,72], or by HNO<sub>2</sub> + NO<sub>2</sub> → HNO<sub>3</sub> + NO (under conditions with a large excess of NO<sub>2</sub>) [71]. Either of these subsequent reactions will lead to the stoichiometry of 3NO<sub>2</sub> + H<sub>2</sub>O → 2 HNO<sub>3</sub> + NO [71], which is often what is written.



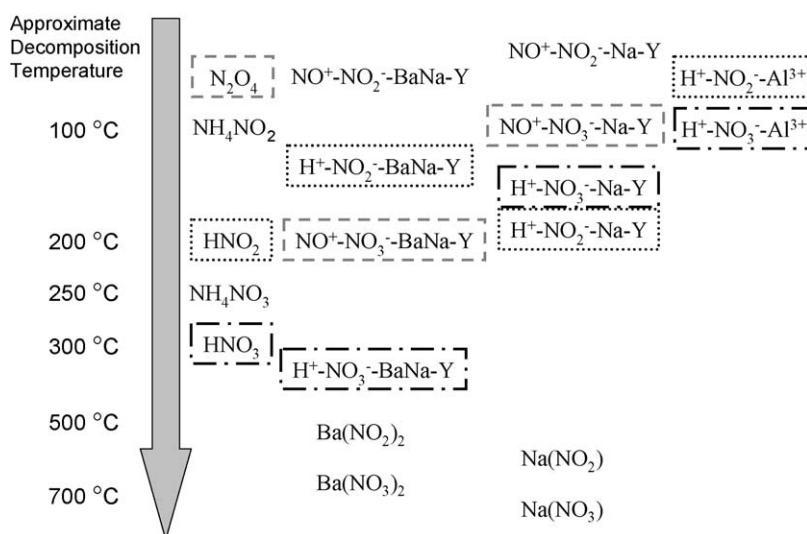


**Fig. 4.** Trends for the approximate stabilities of nitrates and nitrites on BaNa-Y and Na-Y. Boxes indicate groups of nitrates and nitrites with a common counter-ion (e.g., H<sup>+</sup> or NO<sup>+</sup>).

correlated with the specific activity of NO<sub>x</sub> reduction [8], and that Ba<sup>2+</sup> (the most efficient catalyst in this series) has the lowest charge density among the alkaline earth metals [8,38]. The hardness of these adsorption sites could also be influenced by steric hindrance [66], and “site cooperation,” in which more than one site is involved in adsorbate coordination [39,67].

The result is that at these temperatures for NO<sub>x</sub> reduction (200 °C), the critical intermediates of NO<sup>+</sup>–(NO<sub>3</sub><sup>–</sup>)–BaNa–Y and H<sup>+</sup>–(NO<sub>3</sub><sup>–</sup>)–BaNa–Y are stable enough to be reversibly adsorbed and irreversibly adsorbed, respectively, whereas the nitrite species are thermally unstable at these temperatures. This particular mix of stabilities of critical intermediates appears to be among the reasons for the superior performance of BaNa–Y relative to other catalysts in the series, as it follows from the Sabatier principle, that intermediates of a catalytic process should be bound neither too strongly nor too weakly [28].

Kwak et al. [38] and Mignon et al. [39], have shown that the adsorption of nitrates/nitrites can be very sensitive to the method of preparation of the zeolite and its chemical composition. In particular, the influence of acid sites [37,48], silanol groups [19], aluminum cations [19,37,47], Si/Al ratios [32,39], and “cooperation” between sites [39] are not yet elucidated in detail. Szanyi et al. have shown that water may also affect the relative quantities of nitrates and nitrites produced from NO<sub>x</sub> adsorption [17].

The present study suggests that a carefully designed series of experiments may be required to understand how the factors delineated above affect the stabilities of nitrates and nitrites adsorbed on BaNa–Y and related catalysts, and how the stabilities of the nitrates and nitrites are correlated with the activity of these catalysts. The fact that at 200 °C on BaNa–Y, NO<sup>+</sup>–NO<sub>3</sub><sup>–</sup> is adsorbed reversibly, while H<sup>+</sup>–NO<sub>3</sub><sup>–</sup> is adsorbed irreversibly, and both H<sup>+</sup>–NO<sub>2</sub><sup>–</sup> and NO<sup>+</sup>–NO<sub>2</sub><sup>–</sup> are thermally unstable, could be among the reasons for the superior performance of BaNa–Y. Computational modeling [39,68], along with experiments like those in this study, performed in a combinatorial manner, may aid in shedding more light on these issues.

## 5. Conclusions

The kinetics of depletion of chemisorbed surface nitrates and nitrites (H<sup>+</sup>–NO<sub>3</sub><sup>–</sup> and H<sup>+</sup>–NO<sub>2</sub><sup>–</sup>) on Na–Y during TPD were each adequately described by an assumed pre-exponential of 10<sup>13</sup> s<sup>–1</sup> with activation energies for desorption which vary with coverage

from ~100 to 200 kJ mol<sup>–1</sup>. For both the nitrates and the nitrites, with any realistic pre-exponential, the spread of activation energies (the difference between the maximum and minimum of the activation energy curve) is at least 50 kJ mol<sup>–1</sup>. This coverage dependence of the activation energies is likely due to the presence of sets of adsorption sites with different binding energies. The method of preparation of the surface nitrate and nitrite species may affect their relative occupations of shared sites, and thus influence the observed relative stabilities of these surface species.

The relative stabilities of nitrates and nitrites on a given catalyst or two similar catalysts, may play an important role in the hierarchy of catalyst efficiencies observed for alkali/alkaline earth metal Faujasites in low temperature DeNO<sub>x</sub> catalysis. The fact that at 200 °C on BaNa–Y, NO<sup>+</sup>–NO<sub>3</sub><sup>–</sup> is reversibly adsorbed, H<sup>+</sup>–NO<sub>3</sub><sup>–</sup> is irreversibly adsorbed, and both H<sup>+</sup>–NO<sub>2</sub><sup>–</sup> and NO<sup>+</sup>–NO<sub>2</sub><sup>–</sup> are unstable, could be among the reasons for the superior performance of BaNa–Y. The factors which govern these stabilities are not yet fully understood, and will need further study.

However, several trends are clear for alkali and alkaline earth exchanged Na–Y zeolites: (1) nitrates are typically more stable than nitrites; (2) nitrates and nitrites are more stable when H<sup>+</sup> is the counter-ion, than when NO<sup>+</sup> is the counter-ion; (3) the stabilities of nitrates and nitrites are correlated with the adsorption site in the order of: Ba<sup>2+</sup> > Na<sup>+</sup> > Al<sup>3+</sup>.

## Acknowledgments

This work was supported by the Chemical Sciences, Geosciences and Biosciences Division, Office of Basic Energy Sciences, Office of Science, U.S. Department of Energy (DE-FG02-03-ER15457), at the Northwestern University Institute for Catalysis in Energy Processes.

## Appendix A. Supplementary data

Supplementary data associated with this article can be found, in the online version, at doi:10.1016/j.apcatb.2009.02.024.

## References

- [1] F. Klingstedt, K. Arve, K. Eranen, D.Y. Murzin, *Accounts of Chemical Research* 39 (2006) 273–282.
- [2] M.V. Twigg, *Applied Catalysis B* 70 (2007) 2–15.
- [3] M. Koebel, M. Elsener, G. Madia, *Industrial & Engineering Chemistry Research* 40 (2001) 52–59.

- [4] G.T. Panov, M.L. Balmer, C.H.F. Peden, Society of Automotive Engineering, 2001, #2001-2001-3513.
- [5] Y.H. Yeom, B. Wen, W.M.H. Sachtler, E. Weitz, *Journal of Physical Chemistry B* 108 (2004) 5386–5404.
- [6] Y. Yeom, M. Li, A. Savara, W. Sachtler, E. Weitz, *Catalysis Today* 136 (2008) 55–63.
- [7] Y.H. Yeom, M.J. Li, W.M.H. Sachtler, E. Weitz, *Journal of Catalysis* 246 (2007) 413–427.
- [8] J.H. Kwak, J. Szanyi, C.H.F. Peden, *Catalysis Today* 89 (2004) 135–141.
- [9] M.J. Li, Y. Yeom, E. Weitz, W.M.H. Sachtler, *Journal of Catalysis* 235 (2005) 201–208.
- [10] A. Savara, A. Danon, W.M.H. Sachtler, E. Weitz, *Physical Chemistry Chemical Physics* (2008), doi:10.1039/B815605K.
- [11] J. Szanyi, J.H. Kwak, C.H.F. Peden, *Journal of Physical Chemistry B* 108 (2004) 3746–3753.
- [12] P. Basu, T.H. Ballinger, J.T. Yates, *Review of Scientific Instruments* 59 (1988) 1321–1327.
- [13] H. Günzler, H.-U. Gremlich, *IR Spectroscopy: An Introduction*, Wiley-VCH, Weinheim, 2002.
- [14] W. Brügel, *An Introduction to Infrared Spectroscopy*, Wiley, New York, 1962.
- [15] J. Szanyi, J.H. Kwak, R.A. Moline, C.H.F. Peden, *Physical Chemistry Chemical Physics* 5 (2003) 4045–4051.
- [16] C.C. Chao, J.H. Lunsford, *Journal of the American Chemical Society* 93 (1971) 71.
- [17] J. Szanyi, J.H. Kwak, S. Burton, J.A. Rodriguez, C.H.F. Peden, *Journal of Electron Spectroscopy and Related Phenomena* 150 (2006) 164–170.
- [18] G.H. Li, S.C. Larsen, V.H. Grassian, *Journal of Molecular Catalysis A* 227 (2005) 25–35.
- [19] G.H. Li, C.A. Jones, V.H. Grassian, S.C. Larsen, *Journal of Catalysis* 234 (2005) 401–413.
- [20] Y.H. Yeom, J. Henao, M.J. Li, W.M.H. Sachtler, E. Weitz, *Journal of Catalysis* 231 (2005) 181–193.
- [21] N. Shigemoto, S. Sugiyama, H. Hayashi, K. Miyaura, *Journal of Materials Science* 30 (1995) 5777–5783.
- [22] R.I. Masel, *Principles of Adsorption and Reaction on Solid Surfaces*, Wiley, New York, 1996.
- [23] H.G. Karge, V. Dondur, *Journal of Physical Chemistry* 94 (1990) 765–772.
- [24] A.L. Klyachko, *Kinetics and Catalysis* 19 (1978) 983–987.
- [25] J.C. Bruns, *The Surface Chemistry of Several Small Photoactive Molecules Adsorbed on an Insulator Surface Chemistry*, Northwestern University, Evanston, IL, 1990.
- [26] V.P. Zhdanov, J. Pavlicek, Z. Knor, *Catalysis Reviews-Science and Engineering* 30 (1988) 501–517.
- [27] R.C. Baetzold, G.A. Somorjai, *Journal of Catalysis* 45 (1976) 94–105.
- [28] I. Chorkendorff, J.W. Niemantsverdriet, *Concepts of Modern Catalysis and Kinetics*, Wiley-VCH, Weinheim, Germany, 2003.
- [29] H.J. Kreuzer, *Faraday Discussions* (1985) 265–276.
- [30] C. Costa, J.M. Lopes, F. Lemos, F.R. Ribeiro, *Journal of Molecular Catalysis A* 144 (1999) 221–231.
- [31] H.G. Karge, V. Dondur, J. Weitkamp, *Journal of Physical Chemistry* 95 (1991) 283–288.
- [32] N. Cardona-Martinez, J.A. Dumesic, *Advances in Catalysis* 38 (1992) 149–244.
- [33] I.V. Mishin, T.R. Brueva, G.I. Kapustin, *Adsorption* 11 (2005) 415–424.
- [34] T.R. Brueva, A.L. Klyachko, I.V. Mishin, A.M. Rubinshtein, *Kinetics and Catalysis* 20 (1979) 810–814.
- [35] K. Suzuki, N. Katada, M. Niwa, *Journal of Physical Chemistry C* 111 (2007) 894–900.
- [36] K. Suzuki, G. Sastre, N. Katada, M. Niwa, *Physical Chemistry Chemical Physics* 9 (2007) 5980–5987.
- [37] C. Sedlmair, B. Gil, K. Seshan, A. Jentys, J.A. Lercher, *Physical Chemistry Chemical Physics* 5 (2003) 1897–1905.
- [38] J.H. Kwak, J. Szanyi, C.H.F. Peden, *Journal of Catalysis* 220 (2003) 291–298.
- [39] P. Mignon, E.A. Pidko, R.A. Van Santen, P. Geerlings, R.A. Schoonheydt, *Chemistry* 14 (2008) 5168–5177.
- [40] M.J. Li, J. Henao, Y. Yeom, E. Weitz, W.M.H. Sachtler, *Catalysis Letters* 98 (2004) 5–9.
- [41] A. Grossale, I. Nova, E. Tronconi, D. Chatterjee, M. Weibel, *Journal of Catalysis* 256 (2008) 312–322.
- [42] M. Devadas, O. Krocher, M. Elsener, A. Wokaun, N. Soger, M. Pfeifer, Y. Demel, L. Mussmann, *Applied Catalysis B* 67 (2006) 187–196.
- [43] M. Koebel, G. Madia, M. Elsener, *Catalysis Today* 73 (2002) 239–247.
- [44] C. Ciardelli, I. Nova, E. Tronconi, D. Chatterjee, B. Bandl-Konrad, M. Weibel, B. Krutzsch, *Applied Catalysis B* 70 (2007) 80–90.
- [45] I. Nova, C. Ciardelli, E. Tronconi, D. Chatterjee, B. Bandl-Konrad, *Catalysis Today* 114 (2006) 3–12.
- [46] A. Savara, M.J. Li, W.M.H. Sachtler, E. Weitz, *Applied Catalysis B* 81 (2008) 251–257.
- [47] C. Sedlmair, K. Seshan, A. Jentys, J.A. Lercher, *Journal of Catalysis* 214 (2003) 308–316.
- [48] J.H. Kwak, C.H.F. Peden, J. Szanyi, *Catalysis Letters* 109 (2006) 1–6.
- [49] R. Atkinson, D.L. Baulch, R.A. Cox, J.N. Crowley, R.F. Hampson, R.G. Hynes, M.E. Jenkin, M.J. Rossi, J. Troe, *Atmospheric Chemistry and Physics* 4 (2004) 1461–1738.
- [50] M.J. Li, Y.H. Yeom, E. Weitz, W.M.H. Sachtler, *Catalysis Letters* 112 (1) (2006) 29–132.
- [51] A.G. Thaxton, C.C. Hsu, M.C. Lin, *International Journal of Chemical Kinetics* 29 (1997) 245–251.
- [52] W.H. Chan, R.J. Nordstrom, J.G. Calvert, J.H. Shaw, *Environmental Science & Technology* 10 (1976) 674–682.
- [53] W. Tsang, J.T. Herron, *Journal of Physical and Chemical Reference Data* 20 (1991) 609–663.
- [54] R.S. Zhu, M.C. Lin, *Journal of Chemical Physics* 119 (2003) 10667–10677.
- [55] H. Harrison, H.S. Johnston, E.R. Hardwick, *Journal of the American Chemical Society* 84 (1962) 2478–2482.
- [56] H.S. Johnston, L. Foering, R.J. Thompson, *Journal of Physical Chemistry* 57 (1953) 390–395.
- [57] C.M. Kramer, Z.A. Munir, J.V. Volponi, *Solar Energy Materials* 6 (1981) 85–95.
- [58] J.C. Fanning, *Coordination Chemistry Reviews* 199 (2000) 159–179.
- [59] E.S. Freeman, *Journal of Physical Chemistry* 60 (1956) 1487–1493.
- [60] P.K. Gallagher, S.C. Abrahams, D.L. Wood, F. Schrey, R. Liminga, *Journal of Chemical Physics* 75 (1981) 1903–1906.
- [61] X.Y. Chen, J. Schwank, J. Li, W.F. Schneider, C.T. Goralski, P.J. Schmitz, *Applied Catalysis B* 61 (2005) 164–175.
- [62] S. Beran, P. Jiru, B. Wichterlova, *Journal of Physical Chemistry* 85 (1981) 1951–1956.
- [63] A. Chatterjee, T. Iwasaki, T. Ebina, *Journal of Physical Chemistry A* 103 (1999) 2489–2494.
- [64] F. Thibault-Starzyk, O. Marie, N. Malicki, A. Vos, R. Schoonheydt, P. Geerlings, C. Henriques, C. Pommier, P. Massiani, *Studies in Surface Science and Catalysis* 158 (2005) 663–670.
- [65] O. Marie, N. Malicki, C. Pommier, P. Massiani, A. Vos, R. Schoonheydt, P. Geerlings, C. Henriques, F. Thibault-Starzyk, *Chemical Communications* (2005) 1049–1051.
- [66] R.D. Hancock, A.E. Martell, *Journal of Chemical Education* 73 (1996) 654–661.
- [67] K.R.S. Chandrakumar, S. Pal, *Journal of Physical Chemistry A* 106 (2002) 5737–5744.
- [68] C.Y. Sung, L.J. Broadbelt, R.Q. Snurr, *Catalysis Today* 136 (2008) 64–75.
- [69] A. Bambauer, B. Brantner, M. Paige, T. Novakov, *Atmospheric Environment* 28 (1994) 3225–3232.
- [70] Y.N. Lee, S.E. Schwartz, *Journal of Physical Chemistry* 85 (1981) 840–848.
- [71] C. England, W.H. Corcoran, *Industrial & Engineering Chemistry Fundamentals* 13 (1974) 373–384.
- [72] I.R. Mckinnon, J.G. Mathieson, I.R. Wilson, *Journal of Physical Chemistry* 83 (1979) 779–780.